International Research Journal of Engineering Science, Technology and Innovation (IRJESTI) (ISSN-2315-5663) Vol. 2(3) pp. 40-50, March, 2013
Available online http://www.interesjournals.org/IRJESTI

Full Length Research Paper

The method of lines technique in a boundary-fitted curvilinear grid model to simulate 2004 Indian Ocean tsunami

[1]Ashaque Meah M., *[2]Fazlul Karim M., Shah Noor[1] M., [1]Khalid Hossen M. and Pg Md Esa Al-Islam[2]

[1]Department of Mathematics, Shahjalal University of Science and Technology, Sylhet, Bangladesh
[2]Faculty of Engineering, Institute Technology Brunei, Brunei

Accepted March 18, 2013

The boundary-fitted curvilinear grids make the model grids fit to the coastline and the boundary conditions simple and more accurate. Also the method of lines (MOL) is a special finite difference technique which is more effective than the regular finite difference method in terms of accuracy, computational time and numerical stability. So a new numerical solution technique is presented to simulate the 2004 Indian ocean tsunami in a boundary-fitted curvilinear grid model where the vertically integrated shallow water equations are solved by using the method of lines (MOL). For this purpose the boundary-fitted grids are generated along the coastal and island boundaries and the other open boundaries of the model domain. To use the regular finite difference scheme to the spatial derivatives, a transformation is used so that the physical domain is transformed into a rectangular one. The method of lines is then applied to the transformed shallow water equations and the boundary conditions so that the transformed equations are converted into ordinary differential equations initial value problem. Finally the 4th order Runge-Kutta method is used to solve these ordinary differential equations and we use these results for tsunami computation associated with the Indian ocean tsunami 2004 along the west coast of Peninsular Malaysia and Thailand. All simulations show excellent agreement with the observed data.

Keywords: Method of lines (MOL), Boundary fitted curvilinear grid system, Runge-Kutta method, Nonlinear Shallow water equations, Indian Ocean tsunami 2004.

INTRODUCTION

The 26 December 2004 Indian Ocean earthquake which occurred off the west coast of northern Sumatra of Indonesia, triggered a devastating tsunami along the Indian ocean surrounding countries including the west coasts of Peninsular Malaysia and southern Thailand. The tsunami waves spread across the Indian Ocean impacting and causing damage to the shores of more than a dozen countries throughout south and south east Asia. According to Yoon (2002), the prevention and mitigation of tsunami hazards depend on the accurate assessment of the generation, propagation and run-up of tsunamis. So, efforts should be made to construct numerical models. In particular regional tsunami numerical models should be developed as an early warning system. The west coasts of Peninsular Malaysia and southern Thailand are curvilinear in nature and the bending is high along the coasts of these countries (Figure 3). Moreover, there are some offshore islands including Penang in Peninsular Malaysia and Phuket in Thailand. If the coast lines are curvilinear, it is better to use the boundary-fitted grids to represent the model boundaries accurately (Karim et al., 2007; Meah et al., 2011).

Boundary-fitted curvilinear grid systems provide an approach, which combines the best aspects of finite-

*Corresponding Author E-mail: karimfazlul67@gmail.com

difference discretization with grid flexibility. The technique makes the equations and boundary conditions simple and better represents the complex geometry with a relatively less number of grid points and significantly improves the finite difference schemes. But the gridlines of the numerical scheme in boundary fitted curvilinear technique are curvilinear and non-orthogonal and so, regular finite difference scheme can not be applied. The grid system must be rectangular if one wants to use regular finite difference scheme. Hence, the curvilinear boundaries are transformed into straight ones using appropriate transformations, so that the curvilinear physical domain is converted into the transformed rectangular domain where the regular finite difference techniques can be used.

The method of lines (MOL) is a general technique for solving a system of partial differential equations (PDEs) by converting it to a system of ordinary differential equations (ODEs). MOL has long been acknowledged as a very powerful approach to the numerical solution of time dependent partial differential equations (Cash, 2005). It is regarded as a special finite difference method which is more effective than the regular finite difference method in terms of accuracy and computational time (Sadiku and Gorcia, 2000). It has the advantages of less computation time, no relative convergence problem and numerical stability etc (Sun et al., 1993). In the MOL approach, the system of PDEs is converted into a system of ODEs initial value problem by discretizing the spatial derivatives together with the boundary conditions and then the resulting ODEs with time as the independent variable is solved by using a ODE solver.

Karim et al. (2007) developed a shallow water model using a boundary-fitted curvilinear grid system to simulate the 2004 Indonesian tsunami. Izani et al. (2007) developed a stair step numerical scheme based on the MOL for solving the vertically integrated shallow water equations and use this scheme for tsunami computation associated with the 2004 Indonesian. In a stair step model the coastal boundaries are approximated along the nearest finite difference gridlines of the numerical scheme and so the accuracy of a stair step model depends on the grid size. Since very fine resolution was not considered on that stair step model, the representation of the coastal boundaries was not very accurate. In this paper a numerical scheme based on the MOL for solving the shallow water equations in a boundary fitted curvilinear grid system has been developed to simulate the 2004 Indian ocean tsunami along the coast of Peninsular Malaysia and Thailand. For this purpose the west coasts of Malaysia and southern Thailand and the western open sea boundary are represented by two functions. On the other hand, the north and south open sea boundaries were considered as straight lines. In order to generate a set of nonorthogonal curvilinear grid lines in the model domain and the boundary lines two generalized functions are de-fined. Two transformations are used so that the physical domain becomes rectangular. The depth averaged shallow water equations are transformed to the new space domain. The MOL is then applied to these transformed shallow water equations. First, the spetial derivatives of the transformed equations with the boundary conditions are discretized with respect to the spatial variables so that the equations are converted into ordinary differential equations with time as the independent variable and then the each ODE, along with current values of the dependent variables as the initial conditions, are solved by using the classical 4th order Runge-Kutta method to compute the values of the dependent variables at the next instant of time.

Governing Equations and Boundary Conditions

The nonlinear shallow water equations are used here to model the 26 December 2004 Indian ocean tsunami. Let us consider a system of rectangular Cartesian coordinates in which the origin, *O*, is in the undisturbed sea surface (MSL), *x*-axis and *y*-axis are on MSL and *Oz* is directed vertically upwards. The displaced position of the free sea surface from the mean sea level is considered as $z = \zeta(x, y, t)$ and the sea floor as $z = -h(x, y)$ so that, the total depth of the fluid layer is $\zeta + h$. Following Roy (1998), the vertically integrated shallow water equations in flux forms are

$$\frac{\partial \zeta}{\partial t} + \frac{\partial \tilde{u}}{\partial x} + \frac{\partial \tilde{v}}{\partial y} = 0 \quad (1)$$

$$\frac{\partial \tilde{u}}{\partial t} + \frac{\partial (u\tilde{u})}{\partial x} + \frac{\partial (v\tilde{u})}{\partial y} - f\tilde{v} = -g(\zeta + h)\frac{\partial \zeta}{\partial x} - \frac{C_f \tilde{u}\left(u^2 + v^2\right)^{1/2}}{\zeta + h} \quad (2)$$

$$\frac{\partial \tilde{v}}{\partial t} + \frac{\partial (u\tilde{v})}{\partial x} + \frac{\partial (v\tilde{v})}{\partial y} + f\tilde{u} = -g(\zeta + h)\frac{\partial \zeta}{\partial y} - \frac{C_f \tilde{v}\left(u^2 + v^2\right)^{1/2}}{\zeta + h} \quad (3)$$

where, $(\tilde{u}, \tilde{v}) = (\zeta + h)(u, v)$

Here *u* and *v* are the *x* and *y* components of velocity of sea water respectively, g is gravity, *f* is coriolis parameter, C_f is the bottom friction coefficient.

Let *x*-axis and *y*-axis of the model domain are considered towards the west and north directions respentively. The eastern coastal boundary, along *y*-axis, is situated at $x = b_1(y)$ and the western open-sea boundary, parallel to *y*-axis, is at $x = b_2(y)$. The southern open-sea boundary, along *x*-axis, and the northern open-sea boundary, parallel to *x*-axis, are at *y* = 0 and *y* = *L* respectively. This configuration is shown in Figure 1.

Following Roy (1999), the system of gridlines oriented to $x = b_1(y)$ and $x = b_2(y)$ are given by the generalized function

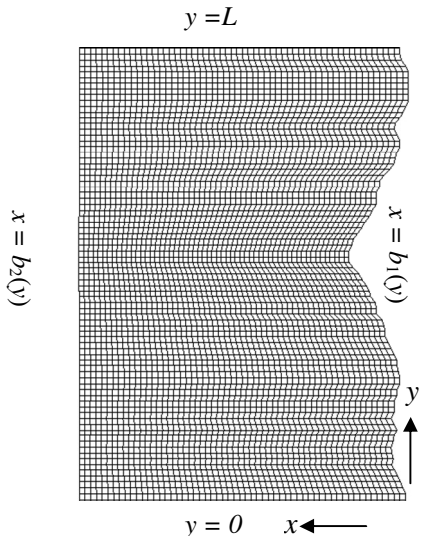

Figure 1. Boundary fitted grids in physical domain.

$$x = \{(k-l)b_1(y) + lb_2(y)\}/k \quad (4)$$

where $k = M$, the number of gridlines in *x*-direction and *l* is an integer and $0 \le l \le k$.

The system of gridlines oriented to $y = 0$ and $y = L$ are given by the generalized function

$$y = \{(q-p)0 + pL\}/q \quad (5)$$

where $q = N$, the number of gridlines in *y*-direction and *p* is an integer and $0 \le p \le q$.

Now by proper choice of *l, k* and *p, q* the boundary-fitted curvilinear grids can be generated. Following Johns et al. (1981), the boundary conditions are given by

$$u - v\frac{db_1}{dy} = 0 \quad \text{at} \quad x = b_1(y), \text{ along } x\text{-axis} \quad (6)$$

$$u - v\frac{db_2}{dy} = (g/h)^{1/2}\zeta \quad \text{at} \quad x = b_2(y), \text{ parallel to } y\text{-axis} \quad (7)$$

$$v + (g/h)^{1/2}\zeta = 0 \quad \text{at } y = 0, \text{ along } x\text{-axis} \quad (8)$$

$$v - (g/h)^{1/2}\zeta = 0 \quad \text{at } y = L, \text{ parallel to } x\text{-axis} \quad (9)$$

To facilitate the numerical treatment of an irregular boundary configuration, a coordinate transformation is introduced, similar to that in Johns et al. (1985), which is based upon new set independent variables η, λ, y, t where

$$\eta = \frac{x - b_1(y)}{b(y)}, \quad \lambda = \frac{y}{L}, \quad b(y) = b_2(y) - b_1(y). \quad (10)$$

This mapping transforms the analysis area enclosed by $x = b_1(y), x = b_2(y), y = 0$ and $y = L$ into a rectangular domain given by $0 \le \eta \le 1, \quad 0 \le \lambda \le 1$ (Figure 2).

The generalized function (4) takes the form

$$\eta = \frac{l}{k}. \quad (11)$$

The generalized function (5) takes the form

$$\lambda = \frac{p}{q}. \quad (12)$$

By the proper choice of the constants *k* and *q* and the parameters *l* and *p*, rectangular grid system can be generated in the transformed domain.

By using the transformations (10), and taking η, λ, y, t as the new independent variables, the equations (1) – (3) transform to (Karim et al., 2007)

$$\frac{\partial(bL\zeta)}{\partial t} + \frac{\partial \tilde{U}}{\partial \eta} + \frac{\partial \tilde{V}}{\partial \lambda} = 0 \quad (13)$$

$$\frac{\partial \tilde{u}}{\partial t} + \frac{\partial(U\tilde{u})}{\partial \eta} + \frac{\partial(V\tilde{u})}{\partial \lambda} - f\tilde{v} = -gL(\zeta + h)\frac{\partial \zeta}{\partial \eta} - \frac{C_f \tilde{u}\left(u^2 + v^2\right)^{1/2}}{\zeta + h} \quad (14)$$

$$\frac{\partial \tilde{v}}{\partial t} + \frac{\partial(U\tilde{v})}{\partial \eta} + \frac{\partial(V\tilde{v})}{\partial \lambda} + f\tilde{u} = -g(\zeta + h)\left[b\frac{\partial \zeta}{\partial \lambda} - L\left(\frac{db_1}{dy} + \eta\frac{db}{dy}\right)\frac{\partial \zeta}{\partial \eta}\right] - \frac{C_f \tilde{v}\left(u^2 + v^2\right)^{1/2}}{\zeta + h} \quad (15)$$

where,

$$U = \frac{1}{b}\left[u - \left(\frac{db_1}{dy} + \eta\frac{db}{dy}\right)v\right], \quad V = \frac{v}{L}, \quad (\tilde{u}, \tilde{v}, \tilde{U}, \tilde{V}) = bL(\zeta + h)(u, v, U, V)$$

The boundary conditions (6) – (9) reduces to

$$U = 0 \text{ at } \eta = 0 \quad (16)$$

$$bU - (g/h)^{1/2}\zeta = 0 \text{ at } \eta = 1 \quad (17)$$

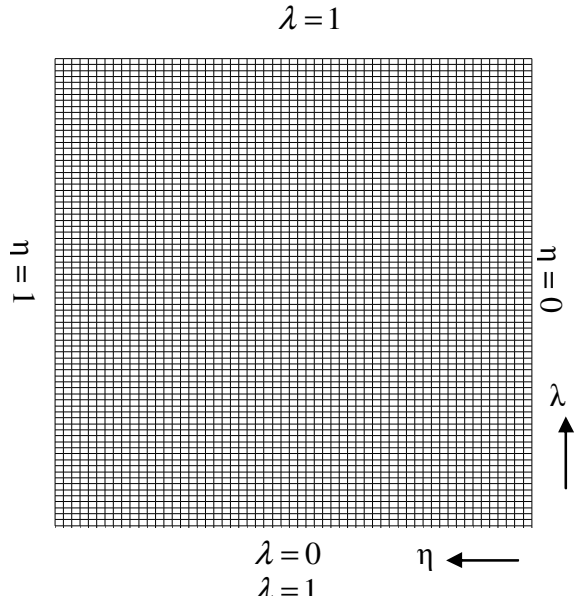

Figure 2. Transformed domain and the rectangular grid lines.

$$VL + (g/h)^{1/2}\zeta = 0 \text{ at } \lambda = 0 \quad (18)$$

$$VL - (g/h)^{1/2}\zeta = 0 \text{ at } \lambda = 1 \quad (19)$$

At each boundary of an island, the normal component of the velocity vanishes. Thus, the boundary conditions of an island are given by

$$U = 0 \text{ at } \eta = l_1/k \text{ and } \eta = l_2/k \quad (20)$$

$$V = 0 \text{ at } \lambda = p_1/q \text{ and } \lambda = p_2/q \quad (21)$$

Implementation of the Method of Lines Scheme and Numerical Discretization

In the MOL approach, a system of partial differential equations (PDEs) is converted into a system of ordinary differential equation (ODE) initial value problem by discretizing the spatial derivatives together with the boundary conditions. This system of ODEs, at every grid point and every instant time, is accompanied by a set of current values (initial values) of the dependent variables at every grid points and its surrounding points. Thus at every grid point and every instant time, we have an initial value problem involving a system of ODE's. The details are discussed in Ismail et, al. (2007).

Now, each ODE of the system, along with current values of the dependent variables as the initial conditions, may be solved by using any of the standard methods to compute the values of the dependent variables at the next instant of time. In this study we will use the classical 4th order Runge-Kutta method.

For convenience of applying the MOL we arrange the transformed equations (13) – (15) in the following form:

$$\frac{\partial \zeta}{\partial t} = -\frac{\partial (\zeta + h)U}{\partial \eta} - \frac{\partial (\zeta + h)V}{\partial \lambda} \quad (22)$$

$$\frac{\partial \tilde{u}}{\partial t} = -\frac{\partial (U\tilde{u})}{\partial \eta} - \frac{\partial (V\tilde{u})}{\partial \lambda} + f\tilde{v} - gL(\zeta + h)\frac{\partial \zeta}{\partial \eta} - \frac{C_f \tilde{u}(u^2 + v^2)^{1/2}}{\zeta + h} \quad (23)$$

$$\frac{\partial \tilde{v}}{\partial t} = -\frac{\partial (U\tilde{v})}{\partial \eta} - \frac{\partial (V\tilde{v})}{\partial \lambda} - f\tilde{u} - g(\zeta + h)\left[b\frac{\partial \zeta}{\partial \lambda} - L\left(\frac{db_1}{dy} + \eta\frac{db}{dy}\right)\frac{\partial \zeta}{\partial \eta}\right] - \frac{C_f \tilde{v}(u^2 + v^2)^{1/2}}{\zeta + h} \quad (24)$$

Since the analysis area or the physical domain is transformed into a rectangular one, the rectangular grid system is generated in the analysis area using a set of equidistant straight lines parallel to η-axis and a set of equidistant straight lines parallel to λ-axis. The space between any two consecutive gridlines parallel to λ-axis is $\Delta\eta$ and that between any two consecutive gridlines parallel to η-axis is $\Delta\lambda$. Let there be *M* gridlines parallel to λ-axis and *N* gridlines parallel to η-axis. So, there are *M* grid points in η-direction and *N* grid points in λ-direction and the total number of grid points is $M \times N$. We define the grid points (η_i, λ_j) in the domain by

$$\eta_i = (i-1)\Delta\eta, \qquad i = 1, 2, 3, \ldots, M \quad (25)$$

$$\lambda_j = (j-1)\Delta\lambda, \qquad j = 1, 2, 3, \ldots, N \quad (26)$$

There are two kinds of independent variables (time and space) in our governing equations. The equations

(22)-(24) together with the boundary conditions (16)-(19) are discretized by finite difference (central) only for space derivatives in the staggered grid system. Thus at a grid point (η_i, λ_j) we obtain only one first order ordinary differential equation involving time derivative of one dependent variable together with values of all dependent variables at the present time instant.

For the purpose of space discretization we use the following notations for conciseness and clarity:

For any dependent variable $\chi(\eta, \lambda, t)$,

$$\chi(\eta_i, \lambda_j, t_k) = \chi^k_{ij}$$

$$\frac{1}{2}(\chi^k_{i+1\,j} + \chi^k_{i-1\,j}) = \overline{\chi^k_{i\,j}}^{\eta}$$

$$\frac{1}{2}(\chi^k_{i\,j+1} + \chi^k_{i\,j-1}) = \overline{\chi^k_{i\,j}}^{\lambda}$$

$$\frac{1}{4}(\chi^k_{i+1\,j} + \chi^k_{i-1\,j} + \chi^k_{i\,j+1} + \chi^k_{i\,j-1}) = \overline{\chi^k_{i\,j}}^{\eta\lambda}$$

For every (η_i, λ_j), where i = 2, 4, . . . , M-2 and j = 3, 5, . . . , N-2, we discretize the space derivatives by centered difference. This means Eq. (22) can be rewritten as

$$\left(\frac{d\zeta}{dt}\right)_{i\,j} = CT1 + CT2 \qquad (27)$$

where

$$CT1 = -\frac{(\zeta^k_{i+1\,j} + h_{i+1\,j})U^k_{i+1\,j} - (\zeta^k_{i-1\,j} + h_{i-1\,j})U^k_{i-1\,j}}{2d\eta}$$

$$CT2 = -\frac{(\zeta^k_{i\,j+1} + h_{i\,j+1})V^k_{i\,j+1} - (\zeta^k_{i\,j-1} + h_{i\,j-1})V^k_{i\,j-1}}{2d\lambda}$$

Eq.(23) can be rewritten as

$$\left(\frac{du}{dt}\right)_{i\,j} = UT1 + UT2 + UT3 + UT4 + UT5 \qquad (28)$$

where

$$UT1 = -\begin{cases} \dfrac{U^k_{i+2\,j}\tilde{u}^k_{i+2\,j} - U^k_{i-2\,j}\tilde{u}^k_{i-2\,j}}{4d\eta}, & for \quad i \neq m-1 \\ \dfrac{\{0.5(3U^k_{m-1\,j} - U^k_{m-3\,j})\}\{0.5(3\tilde{u}^k_{m-1\,j} - \tilde{u}^k_{m-3\,j})\} - U^k_{i-2\,j}\tilde{u}^k_{i-2\,j}}{4d\eta}, \\ for \quad i = m-1 \end{cases}$$

$$UT2 = -\frac{\overline{V^k_{i\,j+1}}^{\eta} * 0.5(\tilde{u}^k_{i\,j} + \tilde{u}^k_{i\,j+2}) - \overline{V^k_{i\,j-1}}^{\eta} * 0.5(\tilde{u}^k_{i\,j} + \tilde{u}^k_{i\,j-2})}{2d\lambda}$$

$$UT3 = f_{i\,j}\overline{\tilde{v}^k_{i\,j}}^{\eta\lambda}$$

$$UT4 = -gL(\zeta^k_{i\,j} + h_{i\,j})\frac{(\zeta^{k+1}_{i+1\,j} - \zeta^{k+1}_{i-1\,j})}{2d\eta}$$

$$UT5 = -\frac{C_f\tilde{u}^k_{i\,j}}{\zeta^{k+1}_{i\,j} + h_{i\,j}}\left[(u^k_{i\,j})^2 + \left(\overline{v^k_{i\,j}}^{\eta\lambda}\right)^2\right]^{1/2}$$

Eq.(24) can be rewritten as

$$\left(\frac{dv}{dt}\right)_{i\,j} = VT1 + VT2 + VT3 + VT4 + VT5 \qquad (29)$$

where

$$VT1 = \begin{cases} \dfrac{\overline{U^k_{i+1\,j}}^{\lambda} * 0.5(\tilde{v}^k_{i\,j} + \tilde{v}^k_{i+2\,j}) - \overline{U^k_{i-1\,j}}^{\lambda} * 0.5(\tilde{v}^k_{i\,j} + \tilde{v}^k_{i-2\,j})}{2d\eta}, & for \quad i \neq 2 \\ \dfrac{\overline{U^k_{i+1\,j}}^{\lambda} * 0.5(\tilde{v}^k_{i\,j} + \tilde{v}^k_{i+2\,j}) - \overline{U^k_{i-1\,j}}^{\lambda} * 0.5(3\tilde{v}^k_{i\,j} - \tilde{v}^k_{i+2\,j})}{2d\eta}, & for \quad i = 2 \end{cases}$$

$$VT2 = \begin{cases} \dfrac{V^k_{i\,j+2}\tilde{v}^k_{i\,j+2} - V^k_{i\,j-2}\tilde{v}^k_{i\,j-2}}{4d\lambda}, & for \quad j \neq 2,\ j \neq n-1 \\ \dfrac{V^k_{i\,j+2}\tilde{v}^k_{i\,j+2} - 0.5(3V^k_{i\,j} - V^k_{i\,j+2}) * 0.5(3\tilde{v}^k_{i\,j} - \tilde{v}^k_{i\,j+2})}{4d\lambda}, \\ for \quad j = 2 \\ \dfrac{0.5(3V^k_{i\,n-1} - V^k_{i\,n-3}) * 0.5(3\tilde{v}^k_{i\,n-1} - \tilde{v}^k_{i\,n-3}) - V^k_{i\,j-2}\tilde{v}^k_{i\,j-2}}{4d\lambda}, \\ for \quad j = n-1 \end{cases}$$

$$VT3 = -f_{i\,j}\overline{\tilde{u}^k_{i\,j}}^{\eta\lambda}$$

$$VT4 = -g(\zeta^k_{i\,j} + h_{i\,j})\left[b_j\frac{\zeta^{k+1}_{i\,j+1} - \zeta^{k+1}_{i\,j-1}}{2d\lambda} - L\left\{\frac{b1_{j+1} - b1_{j-1}}{2dy} + \eta\frac{b_{j+1} - b_{j-1}}{2dy}\right\}\right]$$

$$\frac{(\zeta^{k+1}_{i+1\,j} - \zeta^{k+1}_{i-1\,j})}{2d\eta}$$

$$VT5 = -\frac{C_f\tilde{v}^k_{i\,j}}{\zeta^{k+1}_{i\,j} + h_{i\,j}}\left[\left(\overline{u^k_{i\,j}}^{\eta\lambda}\right)^2 + (v^k_{i\,j})^2\right]^{1/2}$$

Solution of the system of ODE's by fourth order Runge-Kutta method

For every (η_i, λ_j), where i = 2, 4, . . . , M-2 and j = 3, 5, . . . , N-2, Eq. (27) can be written as

$$\left(\frac{d\zeta}{dt}\right)_{i\,j} = F(\zeta^k_{l\,m}, U^k_{l\,m}, u^k_{l\,m}, \tilde{u}^k_{l\,m}, V^k_{l\,m}, v^k_{l\,m}, \tilde{v}^k_{l\,m}, h_{l\,m}) \qquad (30)$$

where $l = i-1, i, i+1$; $m = j-1, j, j+1$. On the right

hand side, $\zeta_{l\,m}^{k}, U_{l\,m}^{k}, u_{l\,m}^{k}, \tilde{u}_{l\,m}^{k}, V_{l\,m}^{k}, v_{l\,m}^{k}, \tilde{v}_{l\,m}^{k}, h_{l\,m}$ are known at the current time and those will be used as the initial conditions for solving Eq. (30) at every time instant.

Similarly for every (η_i, λ_j), where i = 3, 5, . . . , M-1 and j = 3, 5, . . . , N-2, Eq. (28) can be written as

$$\left(\frac{d\tilde{u}}{dt}\right)_{i\,j} = G(\zeta_{l\,m}^{k+1}, U_{l\,m}^{k}, u_{l\,m}^{k}, \tilde{u}_{l\,m}^{k}, V_{l\,m}^{k}, v_{l\,m}^{k}, \tilde{v}_{l\,m}^{k}, h_{l\,m}) \quad (31)$$

where $l = i-2, i-1, i, i+1, i+2$; $m = j-2, j-1, j, j+1, j+2$. On the right hand side, $U_{l\,m}^{k}, u_{l\,m}^{k}, \tilde{u}_{l\,m}^{k}, V_{l\,m}^{k}, v_{l\,m}^{k}, \tilde{v}_{l\,m}^{k}, h_{l\,m}$ are known at the current time and $\zeta_{l\,m}^{k+1}$ is known at one advanced time step and these will be used as the initial conditions for solving Eq. (31) at every time instant.

Finally, for every (η_i, λ_j), where i = 2, 4, . . . , M-2 and j = 2, 4, . . . , N-1, Eq. (29) can be written as

$$\left(\frac{d\tilde{v}}{dt}\right)_{i\,j} = H(\zeta_{l\,m}^{k+1}, U_{l\,m}^{k}, u_{l\,m}^{k}, \tilde{u}_{l\,m}^{k}, V_{l\,m}^{k}, v_{l\,m}^{k}, \tilde{v}_{l\,m}^{k}, h_{l\,m}) \quad (32)$$

where $l = i-2, i-1, i, i+1, i+2$, $m = j-2, j-1, j, j+1, j+2$. On the right hand side, $U_{l\,m}^{k}, u_{l\,m}^{k}, \tilde{u}_{l\,m}^{k}, V_{l\,m}^{k}, v_{l\,m}^{k}, \tilde{v}_{l\,m}^{k}, h_{l\,m}$ are known at the current time and $\zeta_{l\,m}^{k+1}$ is known at one advanced time step and these will be used as the initial conditions for solving Eq. (32) at every time instant.

Now, Eq. (30) together with the so-called initial conditions is solved by the classical 4th order Runge-Kutta method, which is as follows:

$$\zeta_{i\,j}^{k+1} = \zeta_{i\,j}^{k} + \frac{1}{6}(k_1 + 2k_2 + 2k_3 + k_4) \quad (33)$$

where,

$$k_1 = \Delta t F(\zeta_{l\,m}^{k}, U_{l\,m}^{k}, u_{l\,m}^{k}, \tilde{u}_{l\,m}^{k}, V_{l\,m}^{k}, v_{l\,m}^{k}, \tilde{v}_{l\,m}^{k}, h_{l\,m}),$$

$$k_2 = \Delta t F(\zeta_{l\,m}^{k} + \frac{1}{2}k_1, U_{l\,m}^{k}, u_{l\,m}^{k}, \tilde{u}_{l\,m}^{k}, V_{l\,m}^{k}, v_{l\,m}^{k}, \tilde{v}_{l\,m}^{k}, h_{l\,m}),$$

$$k_3 = \Delta t F(\zeta_{l\,m}^{k} + \frac{1}{2}k_2, U_{l\,m}^{k}, u_{l\,m}^{k}, \tilde{u}_{l\,m}^{k}, V_{l\,m}^{k}, v_{l\,m}^{k}, \tilde{v}_{l\,m}^{k}, h_{l\,m}),$$

$$k_4 = \Delta t F(\zeta_{l\,m}^{k} + k_3, U_{l\,m}^{k}, u_{l\,m}^{k}, \tilde{u}_{l\,m}^{k}, V_{l\,m}^{k}, v_{l\,m}^{k}, \tilde{v}_{l\,m}^{k}, h_{l\,m}),$$

and where $l = i-1, i, i+1$; $m = j-1, j, j+1$

After updating the values of ζ at the interior points at each time step, the boundary conditions (17) – (19) are used to update values of ζ at the boundary points.

Next, the solution of Eq. (31) is obtained as follows:

$$\tilde{u}_{i\,j}^{k+1} = \tilde{u}_{i\,j}^{k} + \frac{1}{6}(k_1 + 2k_2 + 2k_3 + k_4) \quad (34)$$

where,

$$k_1 = \Delta t G(\zeta_{l\,m}^{k+1}, U_{l\,m}^{k}, u_{l\,m}^{k}, \tilde{u}_{l\,m}^{k}, V_{l\,m}^{k}, v_{l\,m}^{k}, \tilde{v}_{l\,m}^{k}, h_{l\,m})$$

$$k_2 = \Delta t G(\zeta_{l\,m}^{k+1}, U_{l\,m}^{k}, u_{l\,m}^{k}, \tilde{u}_{l\,m}^{k} + \frac{1}{2}k_1, V_{l\,m}^{k}, v_{l\,m}^{k}, \tilde{v}_{l\,m}^{k}, h_{l\,m})$$

$$k_3 = \Delta t G(\zeta_{l\,m}^{k+1}, U_{l\,m}^{k}, u_{l\,m}^{k}, \tilde{u}_{l\,m}^{k} + \frac{1}{2}k_2, V_{l\,m}^{k}, v_{l\,m}^{k}, \tilde{v}_{l\,m}^{k}, h_{l\,m})$$

$$k_4 = \Delta t G(\zeta_{l\,m}^{k+1}, U_{l\,m}^{k}, u_{l\,m}^{k}, \tilde{u}_{l\,m}^{k} + k_3, V_{l\,m}^{k}, v_{l\,m}^{k}, \tilde{v}_{l\,m}^{k}, h_{l\,m})$$

and where $l = i-2, i-1, i, i+1, i+2$; $m = j-2, j-1, j, j+1, j+2$

Finally, the solution of Eq. (32) is obtained as follows:

$$\tilde{v}_{i\,j}^{k+1} = \tilde{v}_{i\,j}^{k} + \frac{1}{6}(k_1 + 2k_2 + 2k_3 + k_4) \quad (35)$$

where,

$$k_1 = \Delta t H(\zeta_{l\,m}^{k+1}, U_{l\,m}^{k}, u_{l\,m}^{k}, \tilde{u}_{l\,m}^{k}, V_{l\,m}^{k}, v_{l\,m}^{k}, \tilde{v}_{l\,m}^{k}, h_{l\,m})$$

$$k_2 = \Delta t H(\zeta_{l\,m}^{k+1}, U_{l\,m}^{k}, u_{l\,m}^{k}, \tilde{u}_{l\,m}^{k}, V_{l\,m}^{k}, v_{l\,m}^{k}, \tilde{v}_{l\,m}^{k} + \frac{1}{2}k_1, h_{l\,m})$$

$$k_3 = \Delta t H(\zeta_{l\,m}^{k+1}, U_{l\,m}^{k}, u_{l\,m}^{k}, \tilde{u}_{l\,m}^{k}, V_{l\,m}^{k}, v_{l\,m}^{k}, \tilde{v}_{l\,m}^{k} + \frac{1}{2}k_2, h_{l\,m})$$

$$k_4 = \Delta t H(\zeta_{l\,m}^{k+1}, U_{l\,m}^{k}, u_{l\,m}^{k}, \tilde{u}_{l\,m}^{k}, V_{l\,m}^{k}, v_{l\,m}^{k}, \tilde{v}_{l\,m}^{k} + k_3, h_{l\,m})$$

and where $l = i-2, i-1, i, i+1, i+2$; $m = j-2, j-1, j, j+1, j+2$

Model Data Set-up

The η-axis is directed towards west at an angle 15° (anticlockwise) with the latitude line and the λ-axis is directed towards north inclined at an angle 15° (anticlockwise) with the longitude line. In this model the analysis area is extended from 2° N to 14° N latitudes (incorporating the west coasts of Malaysia including Penang and Southern Thailand including Phuket) and 91° E to 100.5° E longitudes (Figure 3) which includes the tsunami source region associated with 2004 Indonesian tsunami. The origin of the Cartesian coordinate system is at O (3.125° N, 101.5° E). The number of grids in η and λ- directions are respectively M = 230 and N = 319 so that there are 73370 grid points. The time step is set to 10s in this computation and no stability problem was observed. Following Kowalik et al. (2005), the value of the friction coefficient C_f is taken as 0.0033 through out the model area. The available depth data for some representative grid points of the model area are collected from the Admiralty bathymetric charts. The depth at the entire rest grid points of the mesh are computed by some averaging process. The bathymetry of the modal domain is shown in the Figure 4.

Tsunami Source Generation and Initial Conditions

The tsunami generation is modelled by the initialisation of

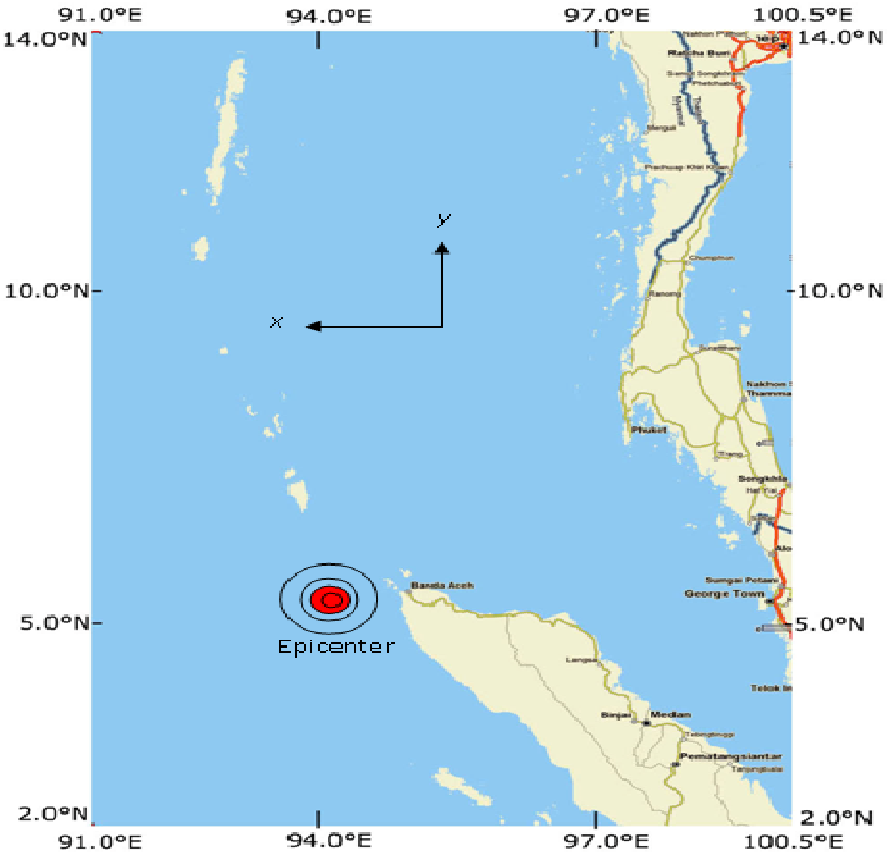

Figure 3. Model Domain including the coastal geometry and the epicenter of the 2004 earthquake (Courtesy: Roy et al., 2006).

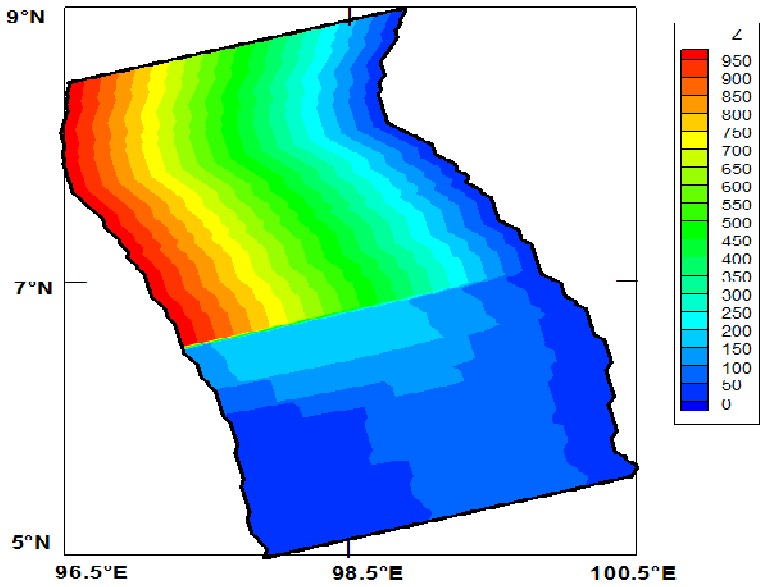

Figure 4. Bathymetry used in the numerical simulation (depth unit: m).

the water surface. The generation mechanism of the 26 December 2004 tsunami was mainly due a static sea floor deformation caused by an abrupt slip at the India/Burma plate interface. Kowalik et al. (2005) des-

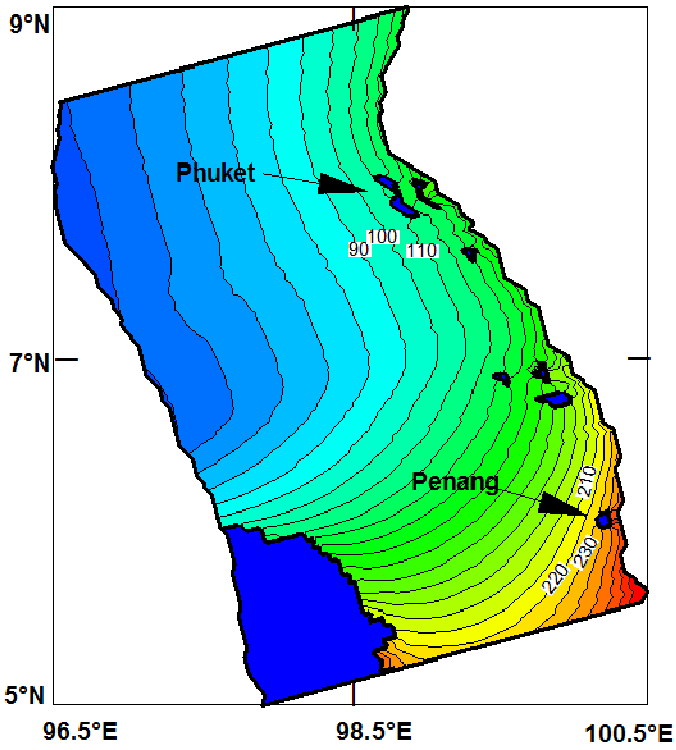

Figure 5. Tsunami propagation time in minutes towards Phuket and Penang.

cribed that the estimated uplift and subsidence zone of the 2004 Indian ocean earthquake is between 92° E to 97°E and 2°N to 10°N with a maximum uplift of 507 cm at the west and maximum subsidence of 474 cm at the east so that the uplift to subsidence is approximately from west to east relative to the west coasts of the Malaysian Peninsula and Thailand. We assume that this sea surface displacement is the same as the ocean bottom displacement, due to incompressibility of the ocean. We consider the source zone extended along the fault line same as Kowalik et. al. (2005) and the disturbance in the form of rise and fall of sea surface is assigned as the initial condition in the model with a maximum rise of 5 m to maximum fall of 4.75 m to generate the response along the western open boundary. In all other regions the initial sea surface deviations are taken as zero. Also the initial *x* and *y* components of the velocity are taken as zero throughout the model area.

Simulation of 2004 Tsunami through the Method of Lines

We studied the propagation of tsunami wave along the coastal belts of Peninsular Malaysia and southern Thailand. Tsunami travel time and water levels at different coastal locations are also presented.

Tsunami travel time to the given location from the source region is an important parameter in the tsunami prediction and warning. The numerical computation of tsunami travel time at every grid points are presented in Figure 5 which shows the contour plot of time, in minutes, for attaining +0.1 m sea level rise at each grid point in the model domain. Thus considering the 0.1 m sea level rise as the arrival of tsunami, it is seen that after generating initial tsunami wave at the source region, the disturbance propagates gradually towards the Penang and Phuket coast. The computed tsunami travel times show that the tsunami travel times to Phuket and Penang Islands are approximately 110 and 230 minutes. According to United States Geological Survey (USGS) report the tsunami waves reached at Phuket within two hours time after the earthquake. The USGS website data also confirms the fact that the arrival time of tsunami at Penang is between 3 hr 30 min and 4 hours. Hence the computed tsunami travel times long the coastal belts of Peninsular Malaysia and southern Thailand agree well with USGS data.

Figure 6 shows the distribution of computed maximum water levels along the west coast of Peninsular Malaysia and Thailand. The maximum water level is from 6 m to 11.5 m approximately at the Phuket region (northern part) of the model area. The tsunami amplitudes are larger in the northwest direction toward Phuket. The maximum coastal surge varies from 18 - 20 m in some locations

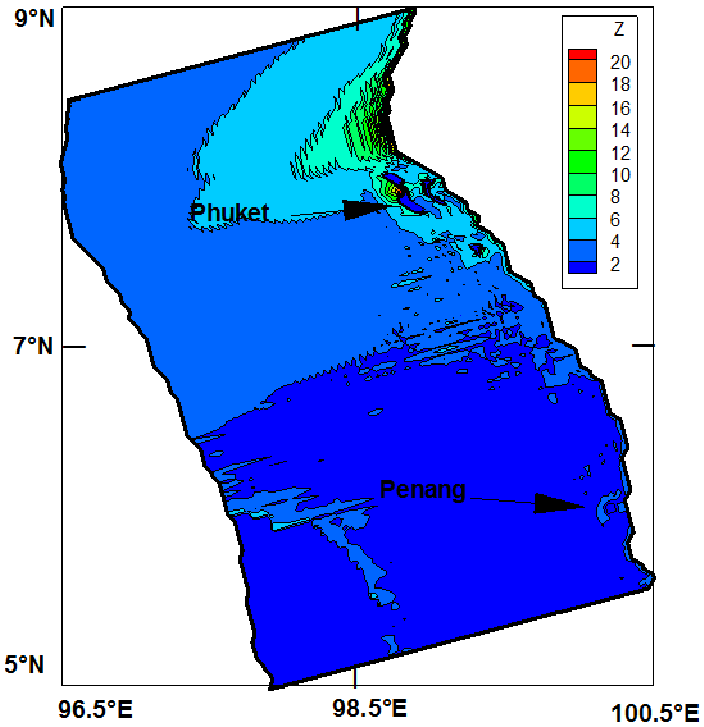

Figure 6. Contour of maximum water elevation around the west coast of Thailand and Malaysia.

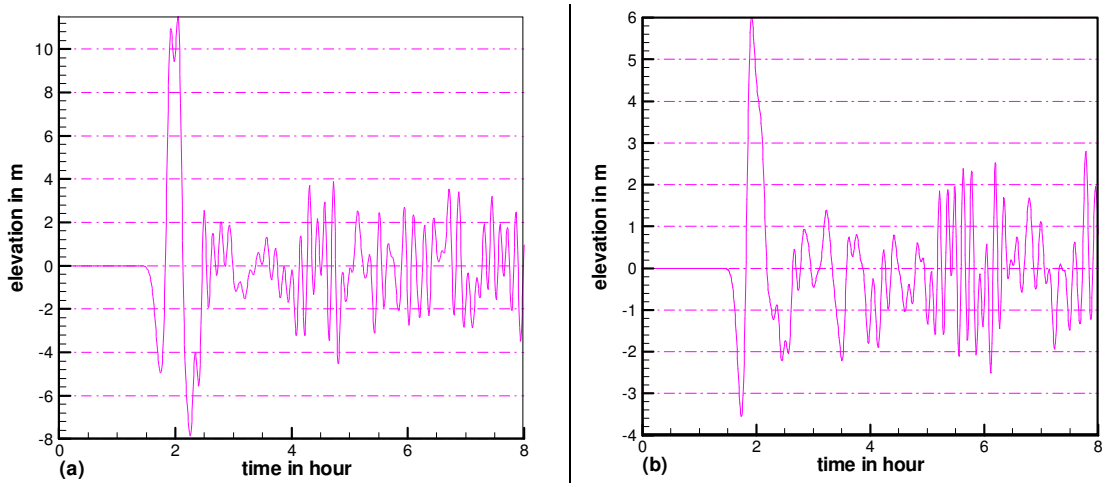

Figure 7. Time histories of water surface fluctuations at two coastal locations of Phuket: (a) West Phuket, (b) South Phuket.

located approximately 50 km north from the Phuket. Tsuji et al. (2006) reported that the largest tsunami height reached up to 19.6 m at Ban Thung Dap located at 50 km north from the Phuket. Thus the model result shows a quite good agreement with the study of Tsuji et al. (2006) for the Phuket region. The computed tsunami amplitudes are relatively smaller along the Penang coast. The maximum amplitudes at Penang Island are ranging from 2 m to 3.5 m with an increasing trend towards the north. The north and west coast is found to be vulnerable for stronger tsunami surge. On the east coast, the measured tsunami heights show a decreasing trend towards the north.

The computed time histories of water surface fluctuations for the source of Indonesian tsunami 2004 at different locations of the coastal belt of Phuket and Penang are stored at an interval of 30 seconds. Figure 7 depicts the time series of water levels for the Phuket

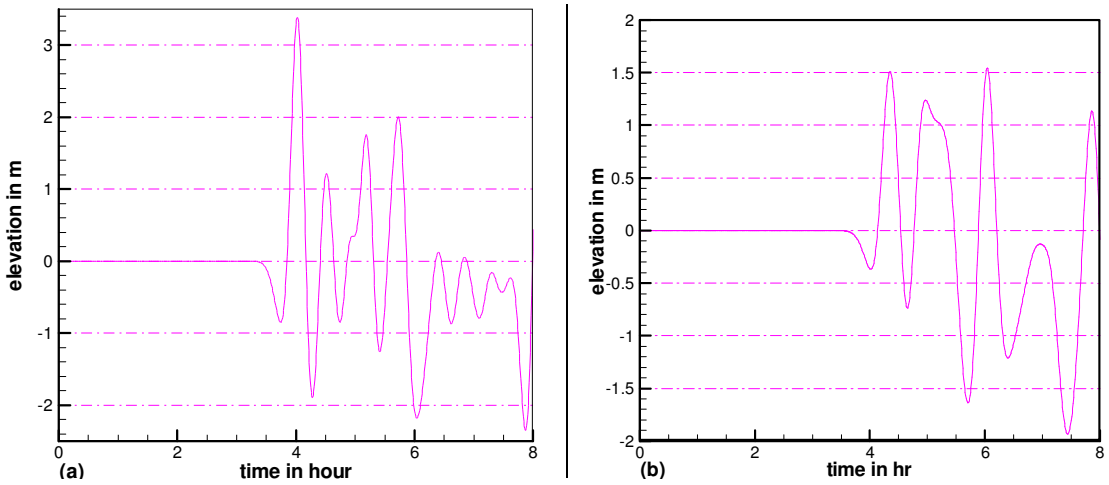

Figure 8. Time histories of water surface fluctuations at two coastal location of PenangIsland: (a) North-West coast, (b) South coast.

Table 1. Computed and observed / USGS tsunami propagation time and water levels for Penang and Phuket.

		MOL in Boundary-Fitted	MOL in Stair Step	Boundary-Fitted	USGS
Propagation time (min)	Penang	230	240	240	< 240
	Phuket	110	90	110	< 120
Max. water level (m)	surrounding Penang	1.6 - 3.4	2.0 – 3.5	2.0 - 4.0	2.0 – 3.5
	surrounding Phuket	6 – 11.5	5 - 9	6 - 12	7 - 11

region in south west Thailand. At the west coast of Phuket, the maximum water level is 11.5 m and the water level continues to oscillate for long time (Figure 7a). At the south coast of Phuket the time series begins with a depression of – 3.5 m and the maximum water level reaches up to 6 m (Figure 7b). Figure 8 describes the computed time histories of water surface fluctuations at two locations of Penang Island. At North-West coast the computed amplitudes is up to 3.4 m (Figure 8a) and the computed amplitudes are less than 2 m at the south coast (Figure 8b). In all the locations tsunami comes from the receding sea, and then a large wave arrives; and this corresponds to the observations. The computed results show that, the west coast of Phuket and the north-west coasts of Penang Island are vulnerable for stronger tsunami surges.

The study compares simulated result with two previously developed models: boundary-fitted curvilinear grid model (Karim et al., 2007) and the MOL in stair step model (Ismail et al., 2007) with the USGS data. All the three models have been applied for the same rectangular region between 2^{o} N to 14^{o} N and 91^{o} E to 100.5^{o} E. The models are applied to simulate the propagation of 2004 Indonesian tsunami wave and its arrival time along the coastal belt of Penang and Phuket. In a stair step MOL method the coastal boundaries are approximated along the nearest finite difference gridlines of the numerical scheme and so the accuracy of a stair step model depends on the grid size. In the boundary-fitted curvilinear model the governing equations and the boundary conditions are transformed by using two transformations so that the physical domain are transformed into a rectangular one and the regular finite difference scheme is used to discretized the transformed equations and boundary conditions in the transformed space. The arrival time of tsunami and the maximum water levels computed by the above mentioned three models are compared with the data available in USGS website. (Table 1)

The tsunami travel time for Penang computed by MOL in boundary-fitted curvilinear grid model, MOL in stair step model and boundary-fitted curvilinear models is 230 min, 240 min and 240 min respectively and the travel time for Phuket is 110 min, 90 min and 110 min respectively. In the USGS website it is reported that the tsunami waves reached at Phuket within two hours time after the earthquake and the arrival time of tsunami at Penang is between 3 hr 30 min and 4 hours. Maximum water level surrounding Penang computed by MOL in boundary-fitted curvilinear grid model, MOL in stair step

model and boundary-fitted curvilinear models is 1.6 - 3.4 m, 2.0 – 3.5 m and 2.0 – 4.0 m respectively and the same for Phuket is 6 – 11.5 m, 5 – 9 m and 6 – 12 m respectively. In USGS website it is reported that the maximum water level along Phuket is approximately 7 to 11 m and from post-tsunami survey report it is found that the wave height reached 2.0 – 3.5 m surrounding Penang. From table 1 and above discussion it is clear that the tsunami travel time and maximum water levels along the island boundaries of Penang and Phuket computed by the three models agree well with the observed data or data available in the USGS website. Among the three models results computed from the MOL in boundary-fitted curvilinear grid model shows better agreement with the observed data.

CONCLUSION

In this paper, the method of lines has been applied to solve the vertically integrated shallow water equations with boundary-fitted curvilinear grids to simulate the 2004 Indian ocean tsunami along the coastal belts of Peninsular Malaysia and southern Thailand. As compared with the other tsunami models the simulated results of present model shows better agreement with the USGS and observed data. So the authors do believe that the MOL approach can be applied to a region where the coastal models are strongly affected by boundaries. It is favorable to use this method in the development of regional tsunami early warning system.

REFERRENCES

Cash JR (2005). Efficient time integrators in the numerical method of lines. J. Computational and Appl. Mathematics, vol. 183, 259-274.

Ismail AIM, Karim MF, Roy GD, Meah MA (2007). Numerical Modelling of Tsunami via the Method of lines. Int. J. Mathematical, Physical and Engr Sci., 1(4), 213 - 221.

Johns B, Dube SK, Mohanti UC, Sinha PC (1981). Numerical Simulation of surge generated by the 1977 Andhra cyclone. Quart. J. Roy. Soc. London 107, 919 – 934.

Johns B, Rao AD, Dube SK , Sinha PC (1985). Numerical modelling of tide–surge interaction in the Bay of Bengal. Philos. Trans. R. Soc. London Ser. A, 313, 507–535.

Karim MF, Roy GD, Ismail AIM, Meah MA (2007). A Shallow Water Model for Computing Tsunami along the West Coast of Peninsular Malaysia and Thailand Using Boundary- Fitted Curvilinear Grids. Science of Tsunami Hazards, 26 (1), 21 – 41.

Kowalik Z, Knight W, Whitmore PM (2005). Numerical Modeling of the Tsunami: Indonesian Tsunami of 26 December 2004. Sc. Tsunami Hazards, 23(1), 40 – 56.

Meah MA, Ismail AIM., Karim MF, Islam MS (2011). Simulation of the effect of Far Field Tsunami through an Open Boundary Condition in a Boundary-fitted Curvilinear Grid System. Science of Tsunami Hazards, 31 (1), 1 – 18.

Roy GD (1998). Mathematical Modeling of Tide, Surge and their Interaction along the Coast of Bangladesh. Mini-Workshop on Appl. Math., SUST, Sylhet, Bangladesh.

Roy GD (1999). Inclusion of Off-shore Islands in a Transformed coordinates Shallow Water Model along the Coast of Bangladesh. Environment International, 25(1), 67 - 74.

Sadiku MNO, Gorcia RC (2000). Method of lines solutions of axisymmetric problems. Southeastcon 2000, Proceedings of the IEEE, 7-9. 527-530.

Sun W, Wang YY, Zhu W (1993). Analysis of waveguide inserted by a metallic sheet of arbitrary shape with the method of lines. Int. J. Infrared and Millimeter Waves, 14(10), 2069 - 2084.

Tsuji Y, Namegaya Y, Matsumoto H, Iwasaki SI, Kanbua, W, Sriwichai M , Meesuk V (2006). The 2004 Indian tsunami in Thailand: Surveyed runup heights and tide gauge records. Earth Planets Space, 58(2), 223-232.

Yoon SB (2002). Propagation of distant tsunamis over slowly varying topography. J. Geophysical Res., 107, 1 – 11.